



Optical, Acoustical, and Fine Root Analyses of Emerald Ash Borer Infested Ash Trees

By Anand Persad, Gregory Ames Dahle, David DeVallance,
Oscar J. Rocha, and Jason Grabosky

Abstract. This study on investigating change in the material properties of ash trees after infestation by emerald ash borer (EAB) (*Agrilus planipennis*) occurred at two locations in northeast Ohio in the summer of 2013. The trees at either site were divided into three groups based on % canopy lost from EAB (group I = 0 to 5%, group II = 6 to 25%, and group III = greater than 40%). A digital image correlation (DIC) system was used to evaluate and compare strain (tissue deformation) on ash branches that were (static) loaded to failure. Stress wave transmission times (T_m) of sound waves through stem wood and fine roots and root balls of the ash trees also were assessed. The DIC evaluations revealed that branches of ash trees that were in groups II and III exhibited significantly lower strain after static loading compared to that observed for trees in group I. Analysis of stress wave T_m revealed that group III trees had significantly higher T_m times compared to the other two groups. Fine root necrosis was significantly higher in group III trees and lowest in group I trees. Extracted root balls from group III trees had significantly higher percentage decay compared to that observed from trees in groups I and II. These data provide fundamental insight into the material properties of ash trees after infestation by EAB and can contribute to arboricultural guidelines for ash tree preservation and help develop safety protocols to address structural loss in trees after EAB infestation.

Keywords. Emerald Ash Borer; Digital Image Correlation; Root Necrosis; Stress Waves.

INTRODUCTION

Since the discovery of the emerald ash borer (EAB), *Agrilus planipennis* Fairmaire, in North America in 2002 in Michigan and Ontario (Cappaert et al. 2005; Poland and McCullough 2006), EAB has expanded its distribution to affect a significant proportion of the ash tree populations in North America. As an urban tree resource, Kovacs et al. (2010) estimate that 37.5 million ash trees in 25 eastern states of the U.S.A. may be affected and have to be removed. Cappaert et al. (2005) estimate ash tree removal associated with EAB infested trees may cost between \$20 and \$60 billion US dollars, while Hauer and Peterson (2016) report on municipalities in affected areas being impacted annually by \$280.5 million US dollars for removal and for preservation efforts. Early detection is crucial to any program geared towards preserving ash trees, and cues that assist monitoring programs in urban settings (e.g., in Persad et al. 2015) may help guide tree preservation efforts. Management choices for treating ash trees after infestation are limited to

relatively narrow windows through which they can be effective. If preservation is not implemented, then the gradual loss of ash tree canopy occurs, resulting ultimately in tree degradation and removal prior to the trees posing unacceptable risk of human injury or property damage (Hauer 2012; Van Natta and Hauer 2012). When working in ash trees that are in decline or killed by EAB, arborist safety and tree stability considerations, especially near targets in urban environments, have received considerable attention. Working in and around EAB infested trees may involve added risk; several studies (Persad et al. 2013, 2015) demonstrate that reduced structural integrity of EAB-infested ash trees occurs well before actual tree death. Arboricultural safety guidance programs will continue to benefit from a growing body of data that investigate further effects of EAB on the whole tree and with focus on stem, branch, and root collar integrity.

At present no data exist on strain mapping of EAB affected branches, stem material properties, root plate

stability, and fine root density of ash trees that are infested with EAB. Recent use of digital image correlation (DIC) software suggests that strain can be mapped remotely (Sebera et al.2014; Sebera et al.2016; Dahle 2017). To resolve this in the context of ash canopy decline (as a visual cue) this study was conducted during the Biomechanics Week of the International Society of Arboriculture (ISA) in August 2013. The 2010 Tree Biomechanics Summit recommended research in understanding the mechanism and mode of tree failures as well as effectiveness of mitigation practices (Dahle et al. 2014).

The study was designed to assist the practitioner with data that could assist in decision making with respect to treat, remove, and/or to estimate the level of risk associated with canopy loss. The study was conducted on three groups of ash trees that had varying levels of canopy loss from infestation by EAB. The first aim was to add to the existing body of knowledge on EAB-infested ash tree branch loading using a DIC stereoscopic photogrammetry system to map strain on branches that were subjected to static loading to failure.

Secondly, a Fakoop acoustics meter was used to compare transmission times of sound waves through the stem wood (Wang et al. 2004a; Dahle et al. 2016) of ash trees in each of the three ash tree groups. Stress waves when generated through wood help to define the physical and mechanical properties of the wood material and may travel at speeds which are dependent on several variables, including direction of travel in the wood in relation to wood grain and fiber, moisture content, and decay incidence (Armstrong 1991; Pellerin 2002; Pellerin 1985).

The third objective focused on the root plate zone and root balls of ash trees in each of the three ash tree groups; root areas were examined for fine root necrosis (root necromass/biomass ratios or N_m/B_m). One technique in assessing fine root production involves assessing the measurements of live (biomass, B_m) and dead (necromass, N_m) amounts of fine roots in terms of dry weights in sequential soil cores (Persson and Stadenburg 2009). Additionally, decay pockets in the root balls were identified and compared for each of three groups of EAB-infested ash trees.

MATERIALS AND METHODS

Green ash (*Fraxinus pennsylvanica* M.) trees at two sites that were first infested with emerald ash borer

(EAB) for at least 2 to 3 years prior to this study were selected for this study in northeast Ohio. Although EAB was present at both sites, ash trees were not uniformly affected and had lost varying amounts of canopy at each of the two sites. Trees at either site were grouped into three groups of 10 trees each, using canopy loss as the main criteria to distinguish the effects of EAB presence: group I – 0 to 5%; group II – 6 to 25%; and group III – > 40%; trees with canopy loss between 25 and 40% were not considered in this trial. The trees in each of the groups occurred in a randomly mixed arrangement within the tree populations at either site.

Green ash trees at the first site (Shalersville, OH: 41.2469° N Latitude, 81.2299° W Longitude) were planted from nursery grown seed stock approximately 30 years ago at site on 4.5 m (14.7 foot) centers (Davey Tree Experts Research Station, Shalersville, OH). Trees at this site ranged from 22.4 to 45 cm (8.8 to 17.7 in) in stem diameter at breast height (dbh).

Green ash trees at the second site grew on the fringe of a pasture in a naturally seeded woodlot (Streetsboro, OH; 41.2392° N Latitude, 81.3459° W Longitude). Trees were estimated from landowner records to be 12 to 15 years old and were varying distances from each other, from 5 m to 6 m (16.4 feet to 19.6 feet). These were smaller trees compared to site one and ranged from 13.5 to 17.2 cm (5.3 to 6.7 in) in stem dbh.

Three methods were used to compare the structural integrity of the three ash tree groups. 1) A stereoscopic photogrammetry digital image correlation (DIC) system was used to evaluate and compare strains on ash branches that were (static) loaded to failure; 2) a Fakoop microsecond timer was used to compare transmission times (T_m μ s/m) of sound waves radially through the pith of stem wood at seven heights; 3) the root plate and root balls of ash trees in each of the three groups were examined for fine root necrosis (root necromass/biomass ratios) and percentage of the surface area of the root ball that was decayed, respectively.

DIC Analysis of Ash Branches with EAB Infestation

Strain (ϵ , relative deformation or change in length of a material, Dahle et al 2017) can be evaluated using a number of standard techniques, which may include the use of strain gauges (example Clairet et al. 2013)

or transducers (Brudi and van Wassenae 2002; Clarie et al. 2006; James and Kane 2008; Kane and Clouston 2008). A more in-depth review of measuring strain in trees can be found in James et al. 2018. Digital image correlation (DIC) algorithms have been used in commercial systems to optically measure deformation; Sebera et al. (2014) used the VIC-3D (Correlated solutions Ltd.) system, while the ARAMIS 3D (GOM GMBH) has been utilized to measure ϵ in wood (e.g., Oscarsson et al. 2014; Dahle et al. 2017). Percent $\epsilon = (L_0 - L_1) / L_0 \times 100$ is calculated by the ARAMIS 3D DIC software, which tracks the spatial movement of the speckles in reference to each other (Windisch et al. 2007; Tanasic et al. 2012), where L_0 is the length before and L_1 length after loading. Unlike strain gauges that can only measure strain at a specific location, DIC can map strain ϵ across the area of interest at the sample, even in the case of irregular geometry, which is often the case in trees. The advantage of stereoscopic photography is that 3D DIC systems can compute displacements and strains on curved surfaces, compared to monoscopic systems which employ a single camera and only compute in-plane deformations (e.g., Windisch et al. 2007; Tanasic et al. 2012; Dahle et al. 2017). A stochastic paint speckling is applied to create a unique series of reference points that can be tracked during testing. This is accomplished by applying black speckling, at the desired size, on top of a white background (Dahle et al. 2017). In this trial, the ARAMIS 3D DIC system was placed on a sturdy scaffolding system which allowed for height placement of the camera to align with the painted branch union (of the branch that was subsequently loaded to failure). We utilized 17 mm lenses, and the DIC system was calibrated to 13 paired images of a $350 \times 280 \text{ mm}^2$ panel to develop a 3-dimensional region for testing. Images were acquired at 2448×2050 pixels with a resolution of 72 pixels per inch. The working distance was 270 cm with a calibration deviation of less than 0.3. The facet size was set to 20×20 pixels with a step size of 15. Linear strain was computed with a 7×7 field with a validity quote of 55.5%. The intersection deviation was maintained below 0.03 which provided an accuracy of $0.03 \pm 0.003\%$. A branch replicate of each of a subset of five trees in each ash tree group was selected for testing based on a defect-free union, no apparent loss of bark over more than 10% of the branch, and an attachment angle within 35 to 60 degrees with the stem.



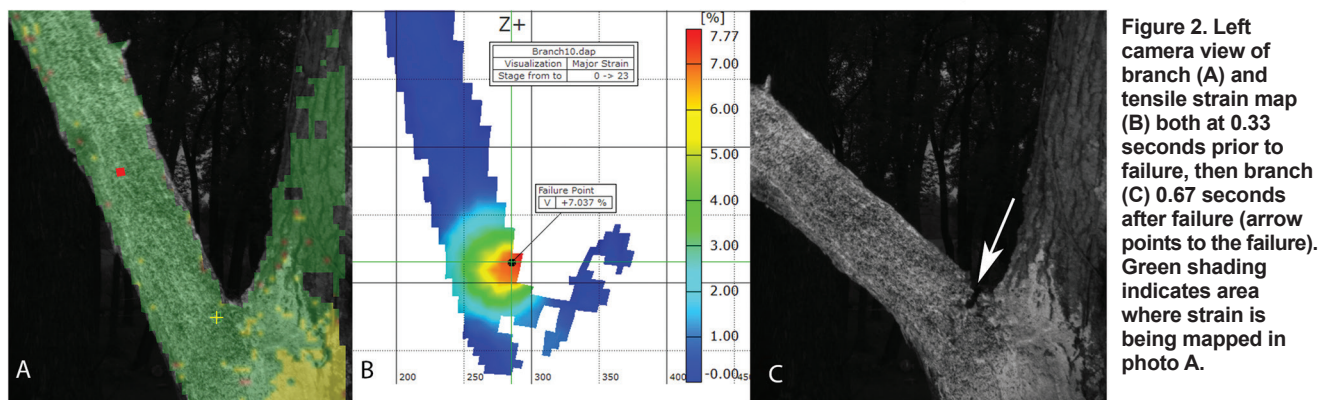
Figure 1. Digital image correlation samples with stereo camera system mounted on a scaffolding. The branch in the background has been painted white with black speckles for strain mapping.

The goal of the static loading was to induce failure and not measure a specific moment arm. The static loading was conducted by attaching a load line to the approximate center of gravity of the selected branch (Persad et al. 2013; Dahle and Grabosky 2012.) The load was applied from a 2 ton battery operated winch until failure occurred and the DIC cameras were focused on the speckled branch section from a side view (Figure 1). During loading and upon ultimate fracture, the strain map was captured in the DIC system at 3 frames per second, and strain maps for each static loading event were captured and analyzed. Major strain (tensile) was measured on the stage just prior to failure (0.33 seconds) at the failure location along the top portion of the branch in the axial direction (Figure 2).

Acoustic Measurements “Transmission Time (T_m)”

Stress wave propagation in standing trees is utilized in forest harvest wood management programs, and the Fakopp 2D Microsecond Timer (FAKOOP Enterprise, H-9423 Agfglva, Fenyo. Str 26 Hungary) used in our study is one standard tool in common use (Wang et al. 2004b) to determine wood quality in standing timber.

Two needles connected to the Fakopp Timer are driven into the bark of the standing tree on opposite sides of the stem and reach the sapwood of the tree;



accelerometers connected to the needles pick up a start and stop signal. A hammer is used to tap one of the sensor needles (start sensor) which generates a stress wave into the tree stem in a radial direction. The opposite sensor works in tandem as a receiver sensor and picks up the stop signal displaying the radial stress wave velocity on an LCD screen (Wang et al. 2004a). The measured transmission times (T_r) values were converted to radial stress wave transmission times (T_m) ($\mu\text{s}/\text{m}$) (example, Mattheck and Bethge 1993; Wang et al. 2004a). In our study, needles were inserted on opposite sides and into the sapwood of the base of each tree and examined from 5 cm (2 in) from the soil line upwards in 15 cm (6 in) increments until 7 readings were obtained (final height near 95 cm [37 in] or close to a meter from the soil line). Five trees in each of the groups were evaluated at both sites. A forestry caliper tool was used to measure the distance (D mm) between the needles at each reading interval, which allowed for the conversion from the transmission time readings (T_r μs) to transmission times (T_m $\mu\text{s}/\text{m}$) using the formula: $T_m = T_r/D$ as described by Wang et al. 2004b.

Root Plate Evaluation

Root Plate Necromass/Biomass (N_m/B_m) Ratios: Soil Cores and Fine Root Analysis to Determine (N_m/B_m) Ratios

Root Plate Necromass/Biomass (N_m/B_m) ratios represent the dead root mass divided by the amount of living root mass determined after examination under the dissecting microscope of fine root tissue taken from the root zones of each replicate tree. Fine roots from trees are pervasive in the soil in and around the root plate zone and are useful indicators of health, as fine

root production improves in suitable site conditions and with tree health (Fontaine et al. 2003). Soil cores of fine roots in this trial were sampled and used as a representation of fine root production under the relatively uniform conditions of soil and topography inherent at the site. Soil cores were taken using a bulk density/slide hammer at the base of each ash tree replicate outwards in five concentric circles. Each progressive circle was a distance equivalent to the stem diameter at breast height further out than the preceding one. Six cores or soil/root samples were randomly taken on each circle, thus thirty cores were collected for each of ten ash tree replicates of the three groups of trees. Core samples were taken to a depth of 20 cm (7.8 in) and individual major roots that cores were extracted from were traced out with an air spade (365 cubic feet per minute) to ensure that samples were taken from correctly identified trees, as roots from adjacent trees often form interlocking root mats. Fine roots in the root cores were extracted from the soil in the laboratory and separated out using a wire mesh sieve (100 nm) and washed gently. The fine roots up to 2 mm were paper dried and were examined under the dissecting scope; each strand was cut longitudinally along the length using a scalpel to identify living and non-living tissue (< 1 mm up to 2 mm). After separating the living roots and dead fine roots, each sample was oven dried at 65° C (149° F) for 24 hours to constant weight (ash/debris excluded, Persson 2012). The dry weights (g) of total fine roots, living fine root tissue (biomass, B_m), and of non-living fine root tissue (necromass, N_m) observed for each core was recorded (Persson and Stadenburg 2010). Comparison of the N_m/B_m ratios were made for 30 soil cores for each ash tree replicate in each of the three ash tree groups.

Root Ball Decay Evaluation

An evaluation of the extent of decay in the root balls of the ash trees in each of the three groups of trees was conducted to investigate root ball decay (if evident) with the extent of canopy loss. The soil surface area around the base of the stem of all trees was cleared of any vegetation or top-laying rocks. Root balls were excavated by first cutting a circle (circumference) with radius that was three times the diameter of the stem at breast height using a diamond edged blade mounted on an industrial concrete cutting saw (48 cm blade). The blade was plunged into the soil and a circular cut was made along the marked circumference. Although at this site the root plates were inundated with small rocks and compacted soil, the full blade depth of 48 cm was achieved for all root balls. The root balls within this volume of earth were excavated using a track Excavator and 48 cm bucket (Mark J. Hoenigman, Busy Bee Services Ltd. Novelty, Ohio). The root balls were power-washed with tap water to remove encrusted soil and air dried. Pockets of decay, if evident on major basal roots (above 2 cm in diameter), were bark traced or the bark around the decay was cut to fully reveal the decay pockets. Percent surface area affected was estimated using a wax paper template placed tightly over the decay zone, marking and measuring the surface area. The overall percentage decay of the root ball was estimated from the ratio of the decay pockets to that of the entire surface area (which was obtained by similarly measuring and recording the surface area of the entire excavated root ball and major roots present; roots < 2 cm were not assessed).

STATISTICAL METHODS

All analyses were conducted in SAS (version 9.1 SAS Institute, Cary, NC). Statistical comparison of means between tree groups were made using the Scheffes test (alpha value = 0.05).

RESULTS AND DISCUSSION

DIC Analysis of Ash Branches with EAB Infestation

Strain at the point of failure after static loading branches to failure was significantly higher (or the change in length upon loading was higher) in group I trees compared to that observed for group II and group III, which were not significantly different from

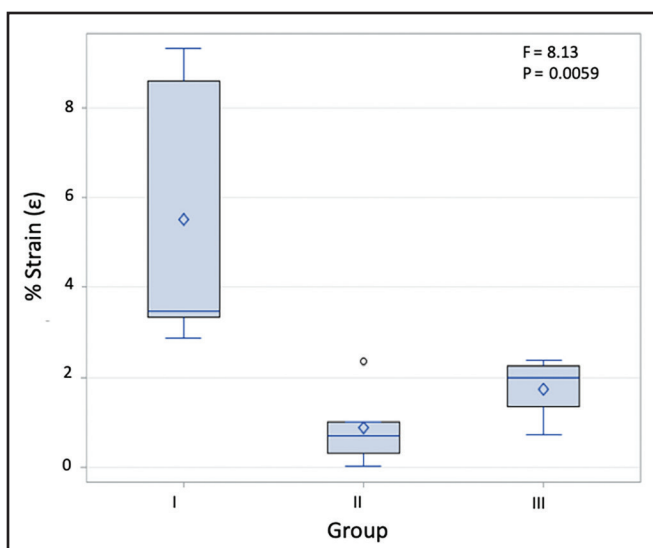


Figure 3. Tensile strain (ϵ) observed in three groups of ash trees infested with EAB (with three levels of canopy loss) after static loading to failure; strain measurements were made using a DIC system. Group I trees (which had most canopy) had branches which exhibited highest strain response compared to that observed for groups II and III which were not significantly different from each other.

each other (Figure 3; $P = 0.0059$, $F = 8.13$, $DF 2, 14$; Scheffes test for Sq Rt Perc. SAS). These data indicate that as canopy loss progresses after infestation with EAB, the strain mapped by DIC decreased significantly with canopy loss (from 6% canopy loss and greater). A decrease in strain could be indicative of less stress required for failure in these branches. Unfortunately, we were not able to measure the applied loading in this study, thus we could not determine stress induced during the testing. Consequently we cannot compare stress and strain at the point of failure.

The incorporation of DIC into this arboricultural research trial is a novel way of using DIC to investigate strains and the effect of a biological entity on wood structural integrity. Further work in utilization of DIC in evaluating how insect and disease pests and other biotic factors may impact tree structure is encouraged. Additionally, the DIC system and strain mapping allows for further understanding of how plants may transfer loading or react during static or dynamic loading (wind, rain, snow, and ice) from one section of tree to another (i.e. from a branch to the central stem) and can help build our arborist safety programs and give insight to tree stability in urban settings.

Acoustic Transmission Time (T_m)

Acoustic transmission time (T_m $\mu\text{s/m}$) observed at site one was not statistically different between groups I and II; group III trees, however, with the most canopy loss had statistically longer T_m $\mu\text{s/m}$ times compared to groups I and II (Figure 4) ($P = 0.0034$, $F = 9.13$, DF 2, 14; Scheffes test for Sq Rt Perc. SAS). Transmission times at site two (smaller trees) increased with canopy loss and was significantly different between all three groups ($P = 0.0052$, $F = 8.53$, DF 2, 14; Scheffes test for Sq Rt Perc. SAS). The mean transmission times obtained in this study for the group I trees are consistent with the range (725 to 861

$\mu\text{s/m}$) recorded by Mattheck and Bethge (1993) and Smulski (1991) (645 to 845 $\mu\text{s/m}$) for healthy standing ash trees. Lower transmission time (higher sound velocity) for group I could be also explained by higher moisture content. Persad et al. (2013) found that trees with similar early canopy loss ranges had significantly higher moisture compared to trees with advanced canopy dieback.

The overall data at both sites indicate that as canopy loss progresses, the transmission times of acoustical stress waves that are perpendicular to the wood grain increase. Pellerin et al. (1985) estimate a 50% decrease in wood structural strength with a 30% increase in transmission time. This study has an average of 33% increase in T_m between group I and group III trees, which may suggest an estimated > 50% in loss of stiffness between trees with < 5% canopy loss compared to trees with > 40% canopy loss. These data are consistent with the findings of an earlier study on static loading (Persad et al. 2013) on decrease in structural strength associated with age of EAB infestation in ash trees.

Root Plate Necromass/Biomass (N_m/B_m) Ratios and Root Ball Decay Evaluation

Root Plate Necromass/Biomass Ratios (N_m/B_m)

From an analysis of N_m/B_m ratios of fine roots observed from soil cores sampled in the three groups of EAB-infested ash trees at site two, group III trees had significantly higher amounts of dead fine roots (Figure 5) compared to groups I and II, which were not significantly different from each other ($P = 0.004$, $F = 9.30$, DF 2, 29; ANOVA Scheffe test, SAS). Fine roots die off for a number of reasons, including reduced carbohydrate supplies, drought, and stresses associated to changes in the soil profile (Reynolds 1970; Marshall and Waring 1985). Reduction in carbohydrate supply to the roots in group III trees may be associated with EAB activity and canopy loss (> 40%), as groups I and II, which had higher N_m/B_m values, were in the same woodlot and were spread randomly amongst the group III trees within the site. The loss of fine roots may also mean the inability to osmo-regulate effectively and could contribute to decay in larger roots. These data that align fine root death with canopy loss can help in tree preservation guidelines, as they may determine if sufficient fine roots are present to facilitate uptake of water and soil applied systemic insecticides and or fertilizers.

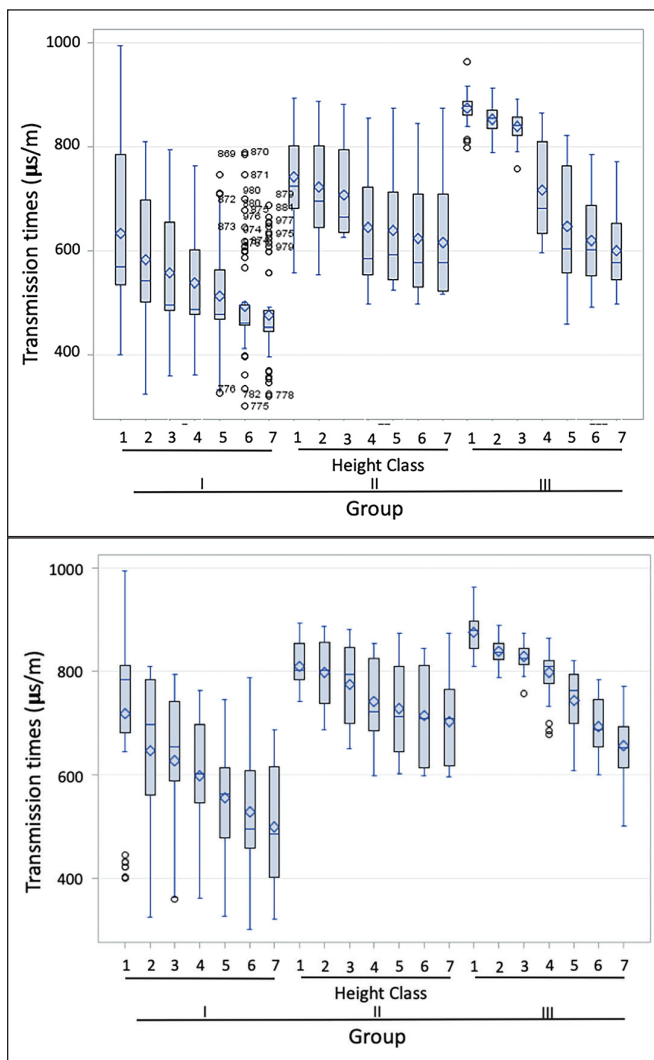


Figure 4. Transmission times (T_m) at site one were significantly higher in group III trees, which had significantly higher T_m times compared to groups I and II, which were statistically similar; at site two for all three groups, T_m times were statistically different ($P < 0.05$) with group III trees having longest and group I shortest T_m times, respectively.

Figure 5. Necromass/Biomass (N_m/B_m) ratios of fine roots observed in the three groups of EAB-infested ash trees (site two) taken from soil cores ($n = 30$); group III trees had the highest amount of dead fine roots compared to groups I and II, which were not significantly different from each other.

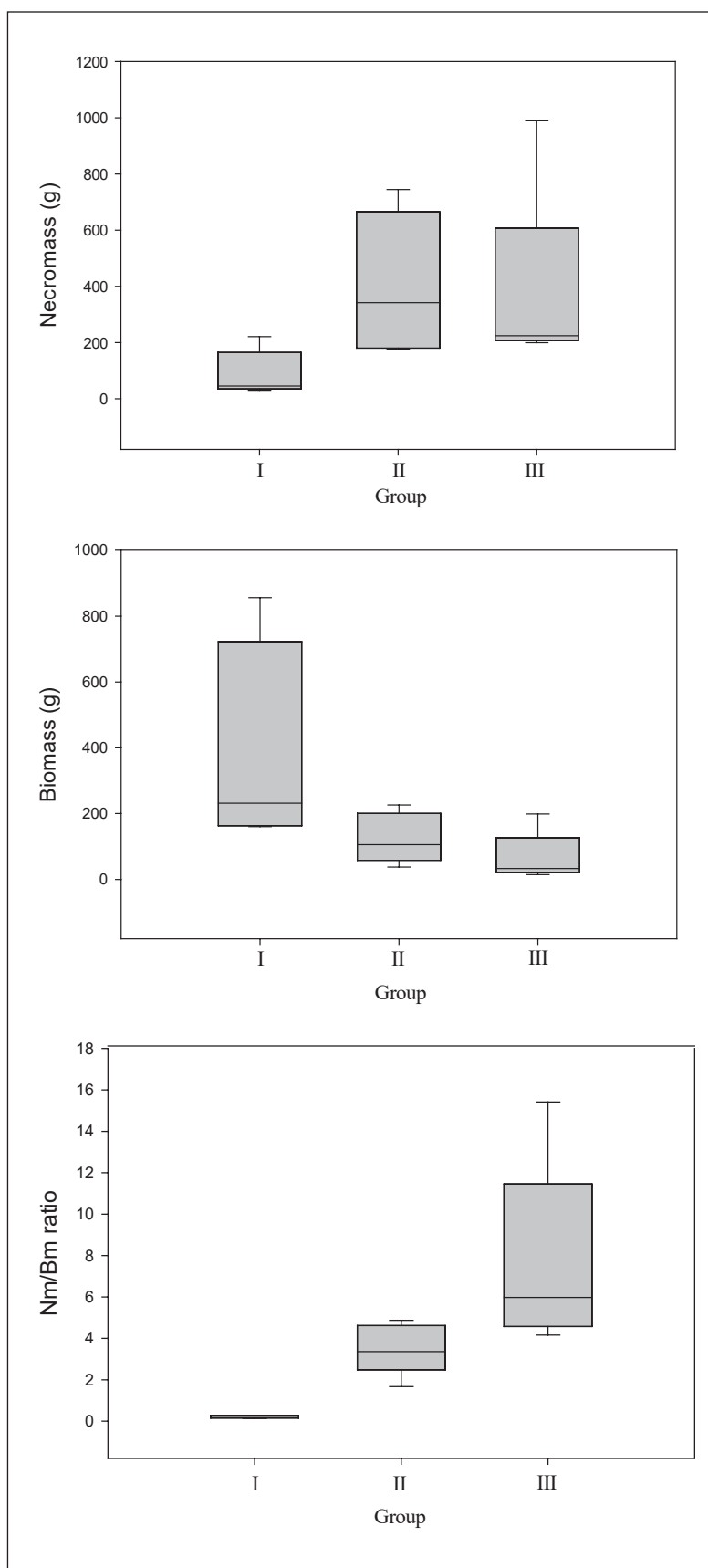
Root Ball Decay Evaluation

Percentage decay in the extracted root balls was significantly different in all groups, with group I trees having the least decay and group III having the highest percentage decay ($P = 0.0002$, $F = 11.64$, $DF 2, 27$; Scheffé's test for Sq Rt Perc. SAS) (Figure 6). Root decay pockets may arise as root tissue is carbohydrate starved and/or is unable to osmo-regulate effectively and may result in water or moisture accumulation and an increase in pathogen activity. These findings on decay incidence with canopy loss can be used in risk evaluation and also provide additional criteria for tree preservation efforts, as root tissue that is compromised may lead to insufficient uptake of water and systemic insecticides resulting in lower efficacy on EAB larvae.

CONCLUSION

The tools used in this trial, the DIC system, stress waves transmission times, and root evaluations of ash trees infested by EAB, provided insight into variation of material properties related to canopy loss. Trees in groups II and III exhibited significantly lower strain during static loading to branch fracture compared to that observed for trees in group I. A decrease in strain could be indicative of less stress required for failure in these branches.

Analysis of stress wave transmission times revealed that at site one (larger trees), group III trees with the highest canopy loss had significantly higher T_m $\mu\text{s}/\text{m}$ times compared to the other two groups. Transmission times increased significantly with advanced canopy loss at site two (smaller trees) between all groups. The use of stress wave technology in evaluating ash tree condition for preservation and other purposes may thus be more apparent in smaller



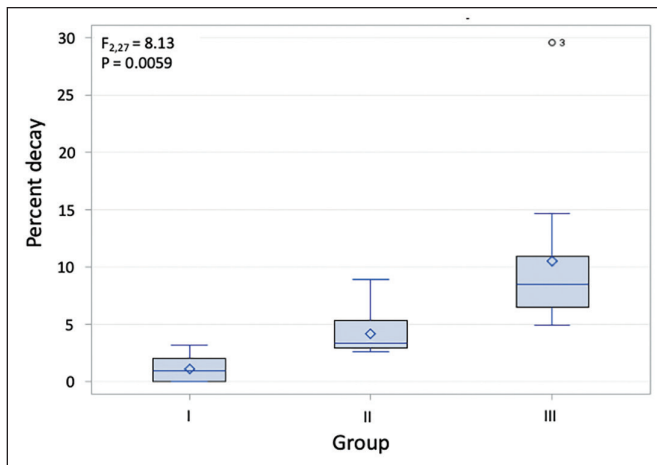


Figure 6. Percent decay of larger roots (> 5 mm) observed in root balls of three groups of ash trees infested with EAB at site two. Percentage decay in the root balls was significantly different in all groups, with group I trees having the least decay and group III having the highest percentage decay.

sized trees. Fine root analyses of the root zone areas (site two) revealed that the N_m/B_m fine root ratios were significantly different between all groups, with group III trees having highest N_m/B_m ratios and group I trees having the lowest. In an evaluation of decay in extracted root balls (site two), group III trees had significantly higher percentage surface area that was decayed compared to groups I and II, which had statistically similar decay incidence. The loss of carbohydrate resources to root tissue with increasing canopy loss may be a factor in the root necromass and decay incidence observed. These data provide fundamental insight into material properties of ash trees after infestation by EAB and can contribute to arboricultural guidelines for ash tree preservation and help develop safety protocols to address structural loss in trees after EAB infestation.

LITERATURE CITED

- Armstrong, J.P., D.W. Patterson, and J.E. Sneckenberger. 1991. Comparison of three equations for predicting stress wave velocity as a function of grain angle. *Wood and Fiber Science* 23(1):32–43.
- Brudi, E., and P. Van Wassenae. 2002. Trees and Statistics: Non-destructive Failure Analysis. In E.T. Smiley and K.D. Coder (Eds.). *Tree Structure and Mechanics Conference Proceedings: How Trees Stand Up and Fall Down*. 53–69.
- Cappaert, D., D.G. McCullough, T.M. Poland, N.W. and Siegert. 2005. Emerald ash borer in North America: a research and regulatory challenge. *American Entomologist* 51:152–165.
- Clair, B., J. Alteyrac, A. Gronvold, J. Espejo, B. Chanson, T. Almeras. 2013. Patterns of Longitudinal and Tangential Maturation Stresses in *Eucalyptus nitens* Plantation Trees. *Annals of Forest Science* 70:801–811.
- Clair, B., J. Ruelle, J. Beauchene, M.F. Prevost, and M. Fournier. 2006. Tension Wood and Opposite Wood in 21 Tropical Rain Forest Species. *IAWA Journal* 27:329–338.
- Dahle, G. 2017. Influence of bark on the mapping of mechanical strain using digital image correlation. *Wood Science and Technology* 51:1469–1477.
- Dahle, G., A. Carpenter, and D. DeVallance. 2016. Non-destructive measurement of the modulus of elasticity of wood using acoustical stress waves. *Arboriculture & Urban Forestry* 42(4):227–233.
- Dahle, G.A., and J.C. Grabosky. 2012. Determining if lateral imbalance exists in first-order branches leading to a potential development of torsional stress. *Arboriculture & Urban Forestry* 38:141–145.
- Dahle, G.A., J. Grabosky, B. Kane, J. Miesbauer, W. Peterson, F.W. Telewski, A. Koeser, and G.W. Watson. 2014. Tree biomechanics: a white paper from the 2010 international meeting and research summit at the Morton Arboretum (Lisile, Illinois, U.S.). *Arboriculture & Urban Forestry* 40:309–318.
- Dahle, G.A., K.R. James, B. Kane, J.C. Grabosky, and A. Detter. 2017. A review of factors that affect the static load-bearing capacity of urban trees. *Arboriculture & Urban Forestry* 43:89–106.
- Fontaine, S., A. Mariotti, and L. Abbadie. 2003. The priming effect of organic matter: a question of microbial competition? *Soil Biology and Biochemistry* 35(6):837–843.
- Hauer, R.J. 2012. Emerald ash borer economics, management approaches, and decision making. *Tree Care Industry* 23(8):14–17.
- Hauer, R.J., and W.D. Peterson. 2016. Effects of emerald ash borer on municipal forestry budgets. *Landscape and Urban Planning*. 157:98–105.
- James, K.R., and B. Kane. 2008. Precision Digital Instruments to Measure Dynamic Wind Loads on Trees During Storms. *Agricultural and Forestry Meteorology* 148:1055–1061.
- James, K.R., J.R. Moore, D. Slater, and G.A. Dahle. 2018. *Tree Biomechanics*. CAB Reviews. doi 10.1079/PAVSNNR201712038.
- Kane, B., and P. Clouston. 2008. Tree Pulling Tests of Large Shade Trees in the Genus *Acer*. *Arboriculture and Urban Forestry* 34:101–109.
- Kovacs, K.F., R.D. Haight, D.G. McCullough, R.J. Mercader, N.A. Seigert, and A.M. Liebhold. 2010. Cost of potential emerald ash borer damage in U.S. communities, 2009–2019. *Ecological Economics* 69(3):569–578.
- Marshall, J.D., and R.H. Waring. 1985. Predicting fine root production and turnover by monitoring root starch and soil temperature. *Canadian Journal of Forest Research* 15(5):791–800.
- Mattheck, C.G., and K.A. Bethge. 1993. Detection of decay in trees with the Metriguard stress wave timer. *Journal of Arboriculture* 19(6):374–378.
- Oscarsson, J., A. Olsson, and B. Enquist. 2012. Strain Fields Around Knots in Norway Spruce Specimens Exposed to Tensile Forces. *Wood Science and Technology* 46:593–610.

- Pellerin, R.F., and R.J. Ross. 2002. Nondestructive evaluation of wood. Madison, WI: Forest Products Society.
- Pellerin, R.F., R.C. DeGroot, and G.R. Esenther. 1985. Nondestructive stress wave measurements of decay and termite attack in experimental wood units. In: Proceedings, 5th Non-destructive testing of wood, 1985. Pullman, WA: Washington State University. 319–353.
- Persad, A.B., and P. Tobin. 2015. Early Detection of the Emerald Ash Borer. *Arboriculture and Urban Forestry* 41(2):103–109.
- Persad, A.B., J. Siefer, R. Montan, S. Kirby, O.J. Rocha, A.W. Jones, C. Ranger, and M. Redding. 2013. Effects of Emerald Ash Borer on the Structure and Material Properties of Ash Trees. *Arboriculture and Urban Forestry* 39:11–16.
- Persson, H.A. 2002. Root system in arboreal plants in Plant Roots—the Hidden Half. Waisel, Y., Eshel, A., and Kafksfi, U. 3: 187–204.
- Persson, H.A. 2012. The high input of soil organic matter from dead tree fine roots into the forest soil. *International Journal of Forestry Research*. 2012(217402).
- Persson, H.A., and I. Stadenberg. 2009. Spatial distribution of fine-roots in boreal forests in eastern Sweden. *Plant and Soil* 318(1–2):1–14.
- Persson, H.A., and I. Stadenberg. 2010. Fine root dynamics in a Norway spruce forest (*Picea abies* [L.] Karst) in eastern Sweden. *Plant and Soil* 330(1):329–344.
- Poland, T.M., and D.G. McCullough. 2006. Emerald Ash Borer: Invasion of the Urban Forest and the Treat to North America's Ash Resource. *Journal of Forestry* 104(3):118–124.
- Reynolds, E.R.C. 1970. Root distribution and the cause of its spatial variability in *Pseudotsuga taxifolia* (Poir.) Britt. *Plant and Soil* 32(1):501–517.
- Sebera, V., J. Kunecky, K. Praus, J. Tippner, and P. Horacek. 2016. Strain Transfer from Xylem to Bark Surface Analyzed by Digital Image Correlation. *Wood Science Technology* 50(4):773–787.
- Tanasic, I., A. Milic-Lemic, L. Tihacek-Soljic, I. Stancic, and N. Mitrovic. 2012. Analysis of the Compressive Strain Below the Removable and Fixed Prosthesis in the Posterior Mandible Using a Digital Image Correlation Method. *Biomechanics and Modeling in Mechanobiology* 11:751–758.
- Vannatta, A.R., R.J. Hauer, and N.M. Schuettpelez. 2012. Economic analysis of emerald ash borer (Coleoptera: Burpres-tidea) management options. *Journal of Economic Entomology* 105(1):196–206.
- Van Wassanaer, P., and A. Persad. 2016. Assessing the Effects of Emerald Ash Borer Infestation on Stem Structural Properties and Uprooting Behavior of Ash Trees. *Tree Fund Canada*.
- Wang, X., R.J. Ross, D.W. Green, B. Brashaw, K. Englund, and M. Wolcott. 2004a. Stress wave sorting of red maple logs for structural quality. *Wood Science Technology* 37:531–537.
- Wang, X., F. Divos, C. Pilon, B.K. Brashaw, R.J. Ross, and R.F. Pellerin. 2004b. Assessment of decay in standing timber using stress wave timing nondestructive evaluation tools. United States Department of Agriculture.
- Windisch, S.I., R.E. Jung, I. Sailer, S.P. Studer, A. Ender, and C.H.F. Hammerle. 2007. A New Optical Method to Evaluate Three-Dimensional Volume Changes of Alveolar Contours: A Methodological in Vitro Study. *Clinical Oral Implants Research* 18:545–551.

ACKNOWLEDGEMENTS

The authors appreciate the help of the volunteers of Biomechanics week 2013. Mark J. Hoenigman assisted with the root ball extractions. We also thank Mike Hannebique, Katie Harper, Josh Gula, and John Siefer for help with various equipment and fieldwork throughout the trials.

Anand Persad (corresponding author)

Davey Institute

Kent, Ohio

United States

anand.persad@davey.com

Gregory Ames Dahle

West Virginian University—Forestry & Natural Resources

Morgantown, West Virginia

United States

David DeVallance

West Virginian University—Forestry & Natural Resources

Morgantown, West Virginia

United States

Oscar J. Rocha

Kent State University—Biology

Kent, Ohio

United States

Jason Grabosky

Rutgers State University of New Jersey

New Brunswick, New Jersey

United States

Résumé. Cette recherche investigate sur les changements des propriétés matérielles des frênes suite à l'infestation par l'agrile du Frêne (AF) (*Agrilus planipennis*) et a été réalisée sur deux sites du nord-est de l'Ohio au cours de l'été 2013. Les arbres de chacun des sites furent répartis en trois groupes en fonction du pourcentage de canopée disparue en raison d'AF (groupe I = 0% à 5%; groupe II = 6% à 25%; groupe III = plus grand que 40%). Une corrélation d'image numérique (CIN) fut utilisée afin d'évaluer et de comparer la déformation des tissus sur les branches de frêne qui étaient alourdies de manière statique jusqu'au point de rupture. Les temps de transition de l'onde de tension (T_m) des ondes acoustiques à travers le bois du tronc, les racines fines et la motte de racines des arbres furent également évalués. Les lectures de CIN révélèrent que les branches de frênes des groupes II et III montrèrent une tension significativement plus basse après chargement statique en comparaison des arbres du groupe I. L'analyse des ondes de tension T_m révéla que les arbres du groupe III montraient une T_m significativement plus élevée que les arbres des deux autres groupes. La nécrose des racines fines était significativement la plus élevée dans les arbres du groupe III et la plus basse dans le groupe I. Suite à leur extraction, les mottes de racines des arbres du groupe III avaient un pourcentage de décomposition du bois significativement plus élevé que celui observé chez les arbres des groupes I et II. Ces données nous procurent un aperçu fondamental des propriétés matérielles des frênes suite à une infestation d'AF et peuvent

contribuer à l'établissement de directives arboricoles pour la préservation des frênes et aider à développer des protocoles de sécurité quant à la perte structurale des arbres consécutivement à une infestation d'AF.

Zusammenfassung. Im Sommer 2013 wurde an zwei Standorten im Nordosten von Ohio eine Studie zur Untersuchung von Veränderungen in den Materialeigenschaften von Eschen nach einer Infektion mit dem Eschenprachtkäfer (EAB) (*Agrilus planipennis*) angefertigt. Die Bäume an jedem Standort wurden in drei Gruppen basierend auf dem Kronenverlust durch EAB eingeteilt: Gruppe I = 0% to 5%, Gruppe II = 6% bis 25%, und Gruppe III = größer als 40%. Es wurde ein digitales Image Korrelationssystem (DIC) verwendet, um die Gewebedeformationen an den Eschenästen, die versagensanfällig waren, zu bewerten und zu vergleichen. Die Zeiten der Stresswellentransmission (T_m) der Soundwellen durch Stammholz, Feinwurzeln und Wurzelballen der Eschen wurde ebenfalls untersucht. Die DIC Bewertungen enthüllten, dass die Äste von Eschen aus den Gruppen II und III wesentlich kleinere Belastungen nach statischem Lasteintrag zeigten als das, was bei den Bäumen in Gruppe I beobachtet wurde. Eine Analyse der Stresswellen T_m zeigte, dass Bäume aus Gruppe III im Vergleich mit den anderen beiden Gruppen signifikant höhere T_m Zeiten aufwiesen. Nekrosen der Feinwurzeln waren in Gruppe III signifikant höher und in Gruppe I am niedrigsten. Ausgegrabene Wurzelballen aus der Gruppe III hatten signifikant höhere Fäuleanteil im Vergleich zu den Beobachtungen aus den Gruppen I und II. Diese Daten liefern fundamentale Einsichten in die Materialeigenschaften von Eschen nach einer Infektion mit EAB und können zu arborikulturellen Richtlinien für den Erhalt von Eschen beitragen und dabei helfen, Sicherheitsprotokolle zu entwickeln, um strukturelle Verluste der Bäume nach einer EAB-Infektion zu bewältigen.

Resumen. Este estudio sobre la investigación del cambio en las propiedades materiales de los árboles de fresno después de la infestación por el barrenador esmeralda del fresno (EAB) (*Agrilus planipennis*) ocurrió en dos lugares en el noreste de Ohio en el verano de 2013. Los árboles en cualquiera de los sitios se dividieron en tres grupos basados en % de pérdida de dosel por EAB (grupo I = 0% a 5%, grupo II = 6% a 25% y grupo III = más del 40%). Se utilizó un sistema de correlación de imágenes digitales (DIC) para evaluar y comparar la tensión (deformación del tejido) en las ramas de fresno que estaban (estáticas) cargadas hasta la falla. También se evaluaron los tiempos de transmisión (T_m) de las ondas de sonido a través de la madera del tallo y las raíces finas y la bola de raíz de los fresnos. Las evaluaciones de DIC revelaron que las ramas de los árboles de fresno que estaban en los grupos II y III mostraron una tensión significativamente menor después de la carga estática en comparación con la observada para los árboles del grupo I. El análisis de la T_m de la onda de estrés reveló que los árboles del grupo III tenían T_m varias veces más altas en comparación con los otros dos grupos. La necrosis de las raíces finas fue significativamente mayor en los árboles del grupo III y más baja en los árboles del grupo I. Las bolas de raíz extraídas de los árboles del grupo III tuvieron un porcentaje significativamente mayor de descomposición en comparación con la observada en los árboles de los grupos I y II. Estos datos proporcionan información fundamental sobre las propiedades materiales de los árboles de fresno después de la

infestación por EAB y pueden contribuir a las directrices de arboricultura para la conservación del árbol de fresno y ayudan a desarrollar protocolos de seguridad para abordar la pérdida estructural en los árboles después de la infestación de EAB.